Electric-field tunable magnetic-field-sensor based on CoFeB/MgO magnetic tunnel junction

V. B. Naik,[a] H. Meng, R. S. Liu,[b] P. Luo, S. Yap, and G. C. Han
*Data Storage Institute, A*STAR (Agency for Science Technology and Research), 5 Engineering Drive 1, DSI Building, Singapore 117608, Singapore*

(Received 21 April 2014; accepted 28 May 2014; published online 9 June 2014)

We demonstrate an electric-field-tunable magnetic-field-sensor based on CoFeB/MgO magnetic tunnel junction with interfacial perpendicular magnetic anisotropy (PMA). From the dynamic lock-in measurements, we show that an applied electric-field induces a peak in sensor voltage (V_{SENSOR}) around the free layer magnetization switching regime in response to external a.c. magnetic field. Detailed measurements of V_{SENSOR} as functions of free layer thickness, a.c. magnetic field amplitude and frequency reveal that the sensitivity of the sensor can be up to 80.8 V cm^{-1} Oe^{-1} under −0.5 V, which can be controlled by the strength and polarity of the applied electric-field via electric-field controlled PMA. We discuss the origin of our observations based on the oscillations in the tunnel magnetoresistance, and this may trigger the development of magnetoelectrically controlled magnetic-field-sensor based on magnetic tunnel junctions. © *2014 AIP Publishing LLC*. [http://dx.doi.org/10.1063/1.4882178]

Voltage-controlled spintronic devices via magnetoelectric (ME) effect is an exciting area of condensed matter research towards developing low-power spintronics technology such as magnetic random access memory (MRAM), magnetic-field-sensor, and spin logic devices.[1–11] The ME effect is generally observed in single-phase multiferroics, which can exhibit simultaneously electric and magnetic orders[1–5,10,11] or in ME composite nanostructures via strain-mediated cross interaction between the magnetostrictive effect in the ferromagnetic phase and piezoelectric effect in the ferroelectric/piezoelectric phase.[12–14] While the ME effect is typically too small in single phase multiferroic materials, it can be much higher in the composite nanostructures. The overall ME properties can be tailored in composite nanostructures by choosing suited materials for both phases, however, they are restricted by the individual properties of the used components. Another limitation of applying these composite nanostructures is the need of external magnetic bias field, which is disadvantageous for any applications such as magnetic sensing or imaging systems requiring a very high sensitivity to a.c. magnetic fields and a high spatial resolution.[14]

Recently, the magnetic tunnel junctions (MTJs) based on CoFeB/MgO with perpendicular magnetic anisotropy (PMA) act as excellent candidates for MRAM, magnetic-field-sensor, logic-in-memory, and microwave oscillator applications due to its high tunneling magnetoresistance (TMR) ratio, faster speed, as well as, lower power consumption.[15–18] The demonstrations of *E*-field controlled PMA and *E*-field assisted switching in perpendicular CoFeB/MgO MTJs at ultralow current density ($J_c \sim 10^4$ A/cm^2) suggests a very promising scheme for achieving low-power consumption spintronic devices.[7–9,19–21] In this work, we report an *E*-field-tunable magnetic-field-sensor based on perpendicular CoFeB/MgO/CoFeB tri-layer MTJ stack by performing dynamic lock-in measurements. We show that a peak in sensor voltage can be resolved around the free layer (FL) magnetization switching regime under the influence of applied d.c. *E*-field. We have carried out detailed measurements of sensor voltage as functions of CoFeB FL thickness, the a.c. magnetic field amplitude and frequency. Our results show that the sensor voltage is very sensitive to the external a.c. magnetic field amplitude and frequency. Also, the sensor voltage shows a strong dependence on the CoFeB FL thickness, and can be tuned by both the strength and polarity of applied *E*-field. The origin of such effects has been discussed based on the oscillations in TMR and *E*-field controlled PMA. Our results of *E*-field-tunable magnetic-field-sensor may be useful for the development of magnetoelectrically controlled magnetic-field-sensor based on MTJs.

The MTJ stacks with structure Si/SiO_2/bottom electrode/Ta2/CoFeB1/MgO2/CoFeB t (thickness) = 1.2–1.7/Ta5/Ru10 (numbers are nominal thicknesses in nanometres), where the composition of CoFeB is $Co_{40}Fe_{40}B_{20}$, were deposited on thermally oxidized Si substrate at room temperature. The multilayer was processed into circular MTJ devices (diameter ∼ 85 nm) by electron beam lithography and ion beam etching processes. The patterned wafer was annealed in a vacuum oven at 300 °C for 1 h. The TMR loops were measured at room temperature with a d.c. voltage (V_{DC}) under a perpendicular scanning magnetic field (H_{DC}). Fig. 1(a) shows the schematic drawing of a MTJ device under external *E*-field (V_{DC}). The positive bias voltage is defined as the tunnelling of electrons from the bottom CoFeB reference layer (RL) to the top CoFeB FL.

To measure the sensitivity of the magnetic-field-sensor properties, a dynamic lock-in method is employed. Fig. 1(b) shows the schematic diagram of the setup used to measure the *E*-field controlled sensor voltage (V_{SENSOR}) across the MTJ device, which is similar to the experimental setup used for ME coefficient measurement as described by Fuentes-Cobas *et al.*[22] An electromagnet was used to generate H_{DC}. The *E*-field (V_{DC}) is applied by using a Keithley's 2602

[a]Email: Vinayak_BN@dsi.a-star.edu.sg
[b]Current address: Western Digital Corp., 44100 Osgood Road, Fremont, CA 94539, US.

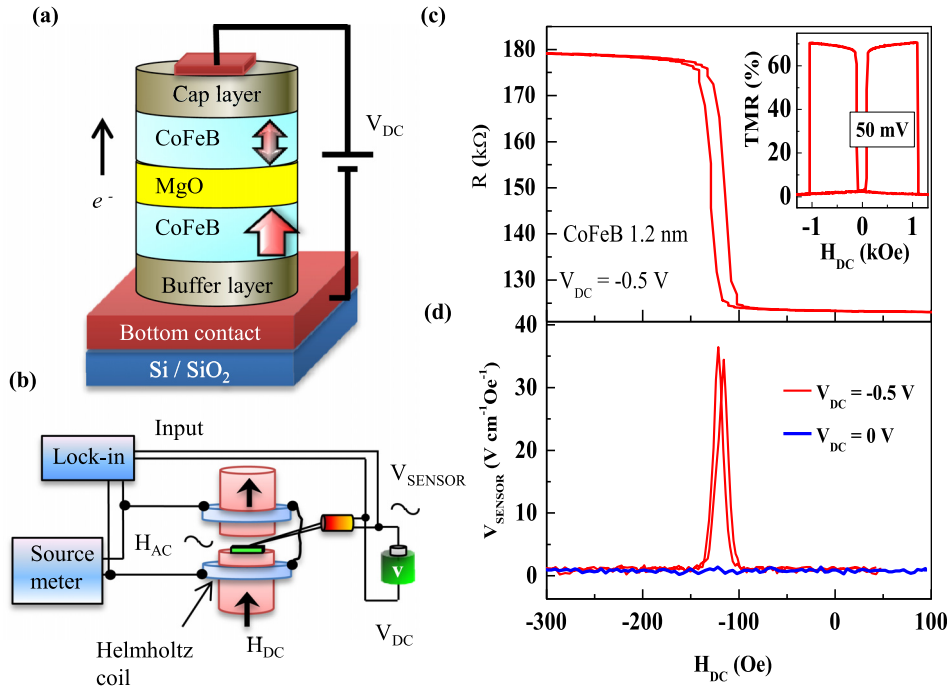

FIG. 1. Electric-field tunable magnetic-field-sensor based on CoFeB/MgO/CoFeB MTJ. (a) Schematic drawing of a MTJ device under external voltage (V_{DC}). The arrow indicates the flow of electrons from the bottom CoFeB (reference layer) to the top CoFeB (free layer). (b) Dynamic lock-in measurement setup to measure the E-field tunable V_{SENSOR} across MTJ device due to the presence of a small a.c. magnetic field (H_{AC}) and d.c. voltage (V_{DC}) under the perpendicular d.c. bias magnetic field (H_{DC}). (c) Minor R-H_{DC} loop of a device with $t = 1.2$ nm at $V_{DC} = -0.5$ V, and the inset shows the full TMR loop at 50 mV with a TMR value of 70%. (d) V_{SENSOR} as a function of H_{DC} at $V_{DC} = 0$ and -0.5 V under $H_{AC} = 1.3$ Oe for $f = 933$ Hz.

source meter. Keithley's 6221 current source was used to drive a pair of Helmholtz coils to generate a.c. magnetic field (H_{AC}) of amplitude 0–1.3 Oe in the frequency range of $f = 0$–5 kHz. An odd value of a.c. magnetic field frequency was chosen for measurements in order to avoid the noise signal which arises from the power line frequency (50 Hz) and also its harmonics. In our measurement configuration, both H_{AC} and H_{DC} are parallel to each other, and both are perpendicular to the plane of MTJ multilayers. The V_{SENSOR} developed across the MTJ device was measured by a lock-in amplifier (SR830, Stanford Research Systems) as a function of H_{DC} at fixed H_{AC} and f. The value of V_{SENSOR} voltage is presented in V cm^{-1} Oe^{-1} using the formula $V_{SENSOR} = \frac{V_{AC}}{[(t_{MgO}+t_{CoFeB})\times H_{AC}]}$, where V_{AC} is the voltage measured by lock-in at its input terminal, and t_{MgO} and t_{CoFeB} are the thicknesses of the MgO and CoFeB layers.

Fig. 1(c) shows the junction resistance (R) of a device with top CoFeB FL of $t = 1.2$ nm as a function of H_{DC} at $V_{DC} = -0.5$ V, which depicts the smooth switching of FL magnetization. The inset shows the full TMR loop at 50 mV with a TMR value of 70%. Fig. 1(d) shows V_{SENSOR} as a function of H_{DC} measured at the optimum frequency of 933 Hz under $H_{AC} = 1.3$ Oe for two voltage bias values, $V_{DC} = 0$ and -0.5 V. A sharp peak is resolved in V_{SENSOR} around the magnetization switching field of FL at $V_{DC} = -0.5$ V, while no peak appears at $V_{DC} = 0$ V. Generally, this kind of peak in induced voltage is observed in ME composite materials that originates from the magnetic-mechanical-electric coupling through the strain transfer across the interface, which is attributed to a sharp change in piezomagnetic coefficient, $q = d\lambda/dH$, where λ is the magnetostriction of magnetostrictive layer in the composite system.[23] However, the appearance of peak in V_{SENSOR} under $V_{DC} = -0.5$ V and its disappearance in $V_{DC} = 0$ reveals that the external E-field is required to induce such voltage in MTJs, and its origin is discussed in the later part of this Letter.

In Fig. 2, we show the evolution of V_{SENSOR} under positive and negative E-field. The map of V_{SENSOR} as functions of negative bias voltages ($V_{DC} = -0.5$ V to 0 V) and H_{DC} is shown in Fig. 2(a), where the H_{DC} is swept from 0 to -300 Oe having the pinned bottom CoFeB RL magnetization pointing upwards. Clearly, there is no sign of any peak in

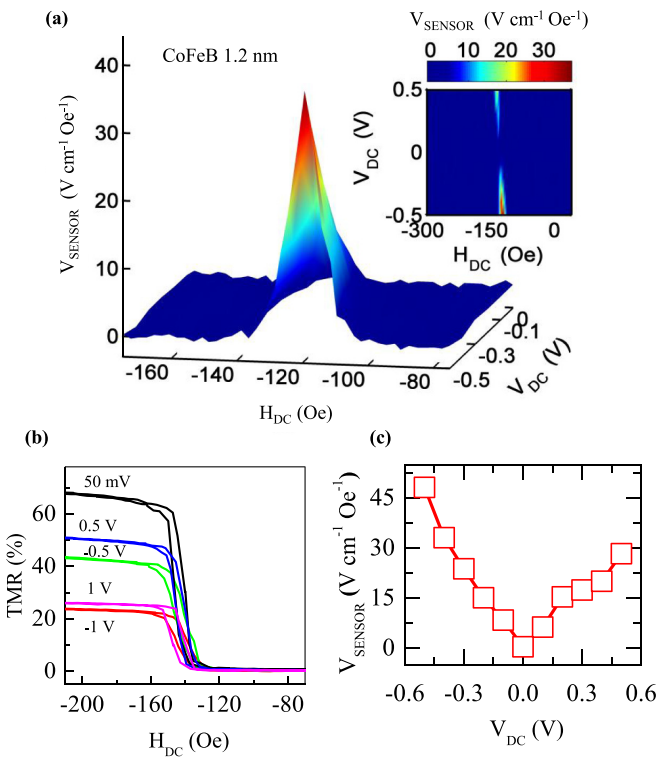

FIG. 2. Evolution of sensor voltage under applied E-field. (a) V_{DC} and H_{DC} map of V_{SENSOR} for different V_{DC} values (0 to -0.5 V). The inset shows the map of V_{DC} and H_{DC} of V_{SENSOR} for $V_{DC} = -0.5$ V to $+0.5$ V. (b) Minor TMR loops of a device with $t = 1.2$ nm at different V_{DC} values (-1 V to 1 V). (c) The peak value of V_{SENSOR} as a function of V_{DC}.

V_{SENSOR} when $V_{DC} = 0$ (no E-field). However, as the magnitude of V_{DC} (E-field) increases, a peak emerges in V_{SENSOR}, and its magnitude also increases with increasing V_{DC}. The inset shows the map of V_{SENSOR} as functions of V_{DC} and H_{DC}, where the magnitudes of the peak under positive bias voltages are slightly lower than that of negative bias voltages. Fig. 2(b) shows the corresponding minor TMR loops at selected V_{DC} values ($V_{DC} = -1$ V to 1 V), which depicts a slight change in slope due to change in PMA under the applied E-field. The PMA change can be more substantial under applied E-field for t close to a critical thickness (t_c—the thickness at which FL magnetization loses its PMA).[24] Fig. 3(c) shows the dependence of peak value of V_{SENSOR} as a function of V_{DC}, which depicts the linear dependence of V_{SENSOR} for both polarities of V_{DC}. A maximum V_{SENSOR} of 36.4 V cm^{-1} Oe^{-1} is obtained for $t = 1.2$ nm under $V_{DC} = -0.5$ V.

A plot of magnitude of V_{SENSOR} as a function of f measured at fixed $H_{AC} = 1.3$ Oe and $V_{DC} = -0.7$ V is shown in Fig. 3(a). The value of V_{SENSOR} increases rapidly and shows a peak around 933 Hz (f_{max}) and then decreases monotonically for $f > f_{max}$. Interestingly, the f_{max} value found in this CoFeB/MgO system is close to the ME resonance frequency of 1197 Hz as reported in CoFeBSi-based ME compound composed of a known piezoelectric material, AlN.[25] The sensitivity of our magnetic-field-sensor is shown in Fig. 3(b), where V_{SENSOR} was measured as a function of H_{AC} at $f_{max} = 933$ Hz and $V_{DC} = -0.7$ V. As can be seen, V_{SENSOR} is detectable even in the small a.c. magnetic field of 0.06 Oe, and its magnitude is linearly increasing with increasing value of H_{AC}, resembling the behavior of a ME sensor made of perfect magnetostrictive and piezoelectric layers.

We have found that the V_{SENSOR} is highly dependent on the angle ϕ between the FL magnetization direction and the applied H_{DC} due to applied E-field. Here, we illustrate the phenomenon by choosing thick ($t = 1.6$ and 1.7, the numbers are nominal thicknesses in nanometres) CoFeB FL such that its magnetization has a crossover point of PMA to in-plane. Figs. 4(a) and 4(c) show the normalized TMR loops measured at 3 selected V_{DC} values for $t = 1.6$ nm and 1.7 nm, respectively. A sharp switching in TMR loop at $V_{DC} = 50$ mV for $t = 1.6$ nm indicates that the FL magnetization has strong PMA (Fig. 4(a)). The PMA of FL becomes stronger under positive bias voltage ($V_{DC} = +1$ V), while it reduces under negative bias voltage ($V_{DC} = -1$ V). Fig. 4(b) shows the evolution of V_{SENSOR} as a function of V_{DC} and H_{DC} at the optimal frequency of 2733 Hz under $H_{AC} = 1.3$ Oe. The V_{SENSOR} signal is observed under negative V_{DC} ($-V_{DC} > -0.2$ V) while V_{SENSOR} is zero under positive V_{DC}. A maximum V_{SENSOR} of 80.8 V cm^{-1} Oe^{-1} is obtained for $t = 1.6$ nm at f_{max} under $V_{DC} = -0.5$ V.

The normalized TMR minor loops for $t = 1.7$ nm at $V_{DC} = 50$ mV is not a sharp rectangular shape (Fig. 4(c)), indicating that the magnetization of FL is tilted which can be clearly seen in the inset where a full TMR loop is shown. The shape of the minor loop changes significantly as the applied V_{DC} changed from -1 V to 1 V, which is due to the tuning of ϕ by V_{DC}, i.e., the negative V_{DC} increases the value of ϕ, while the positive V_{DC} decreases the value of ϕ. Note that the magnetization of FL has not attained a complete PMA, i.e., its magnetization is slightly tilted, even under the maximum positive bias voltage applied ($V_{DC} = 1$ V). In contrast to Fig 4(b), the evolution of V_{SENSOR} is observed only under positive V_{DC} values for $t = 1.7$ nm, and there is no peak in V_{SENSOR} under negative V_{DC}, indicating that the value of V_{SENSOR} is almost negligible for such values of ϕ (Fig. 4(d)).

The origin of a peak observed in the sensor voltage and its dependence on the E-field can be understood from the TMR oscillation and E-field effects. Let us suppose I_{DC} is the d.c. current through the MTJ device when V_{DC} is applied across it. On the application of an a.c. magnetic field of H_{AC}

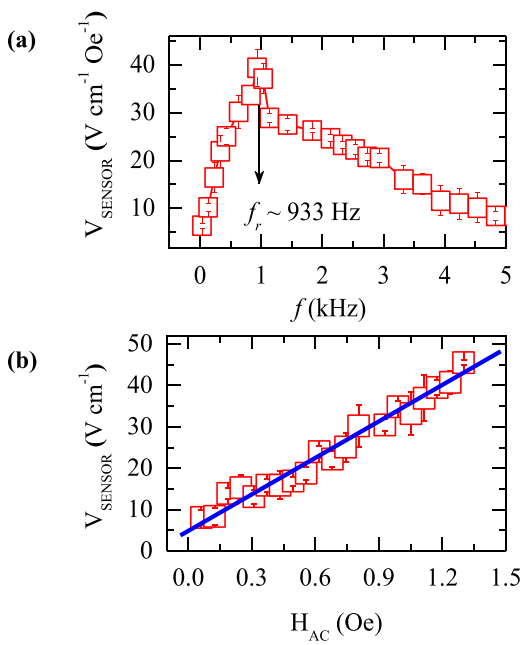

FIG. 3. Sensor voltage response as functions of amplitude and frequency of a.c. magnetic field. (a) The maximum value of V_{SENSOR} as a function of frequency at $H_{AC} = 1.3$ Oe and $V_{DC} = -0.7$ V. The arrow indicates the optimum frequency is around 933 Hz. (b) The maximum value of V_{SENSOR} as a function of magnitude of H_{AC} at $f_{max} = 933$ Hz and $V_{DC} = -0.7$ V. The straight line indicates the linear dependence of V_{SENSOR} with H_{AC}.

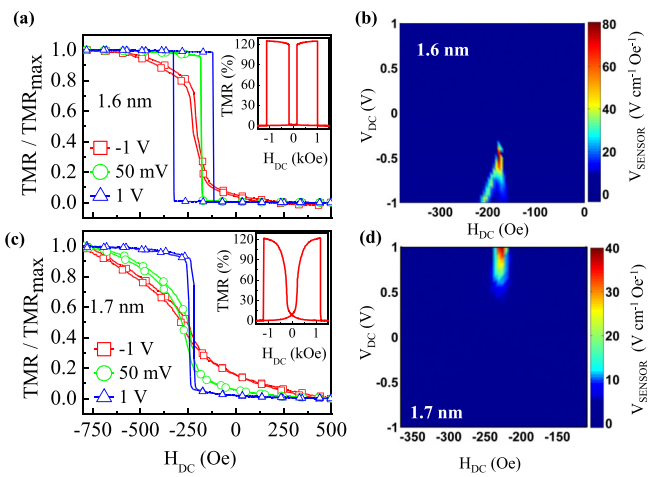

FIG. 4. The effect of E-field on magnetization of thicker CoFeB FL, and its response to sensor voltage. (a) Normalized minor TMR loops at $V_{DC} = 50$ mV, -1 V and $+1$ V for a device with $t = 1.6$ nm having PMA, and (b) shows the V_{DC} and H_{DC} map of V_{SENSOR} at $f_{max} = 2733$ Hz under $H_{AC} = 1.3$ Oe. (c) and (d) show the same for $t = 1.7$ nm having tilted magnetization. The insets in (a) and (c) show the full TMR loops at $V_{DC} = 50$ mV.

onto the device around the FL switching point, the resistance (R) of a MTJ oscillates (R_{AC}) as a function of the d.c. magnetic field because of TMR effect, and is given by $R_{AC} = \frac{dR}{dH_{DC}} \times H_{AC}$. As dR/dH_{DC} attains a maximum value around the FL magnetization switching point, an a.c. voltage is generated from the mixing of I_{DC} and R_{AC} through $V_{AC} = I_{DC} \times R_{AC}$. Since the V_{SENSOR} is calculated based on the value of V_{AC} measured by the lock-in amplifier, V_{SENSOR} is directly proportional to I_{DC}. Therefore, the linear increase in V_{SENSOR} as a function of V_{DC} shown in Fig. 2(c) is in agreement with the mechanism of TMR oscillations.

The dependence of V_{SENSOR} on the angle ϕ between the FL magnetization direction and the applied H_{DC} shown in Fig. 4 is also consistent with the TMR oscillations, which is governed by E-field controlled PMA change. The applied E-field alters the PMA of CoFeB FL such that the positive E-field strengthens the magnetization along the easy axis and the negative E-field tilts the magnetization from the easy axis, corresponding to the sharp and smooth changes in resistance at the magnetization switching point, respectively. As shown in the Fig. 4(a), R-H_{DC} (resistance versus magnetic field) loop for $t = 1.6$ nm has a continuous transition at the FL switching point under the negative bias which leads to a finite dR/dH_{DC} within a certain field range, and thus, the resultant the V_{SENSOR} should be finite and shows a clear peak for negative V_{DC} values (Fig. 4(b)). On the other hand, the resistance changes sharply at the FL switching point under positive bias with a hysteresis in R-H_{DC} loop which leads to dR/R-H_{DC} infinite at those transition points, and equals zero everywhere else. Therefore, no signal was measured in the positive direction (Fig. 4(b)) as the H_{DC} can only have discrete values in the measurements and the transition points can be very easily skipped. A similar situation exists for $t = 1.7$ nm as shown in Figs. 4(c) and 4(d). Although our results can be understood based on the oscillations in the TMR effect, the trend of frequency dependence of V_{SENSOR} is surprising. It resembles the behavior of ME voltage observed in CoFeBSi-AlN based and any other ME composite nanostructures, where a peak in the frequency dependence is observed at the ME resonance frequency.[25] Given that the CoFeB is magnetostrictive with $\lambda_s = 2 \times 10^{-5}$ (where λ_s is the saturation magnetostriction),[23] a peak in frequency dependence of V_{SENSOR} in our CoFeB/MgO MTJ device indicates that it might have some contribution from the ME coupling between the magnetostrictive CoFeB and dielectric MgO layers through strain transfer under the influence of E-field at nanoscale.[26]

In summary, we have demonstrated an E-field-tunable magnetic-field-sensor based on CoFeB/MgO MTJ having interfacial PMA by using dynamic lock-in measurements. From detailed measurements of V_{SENSOR} as functions of CoFeB FL thickness, amplitude, and frequency of H_{AC}, we showed that the sensitivity of the sensor can be achieved up to 80.8 V cm^{-1} Oe^{-1} under -0.5 V, and it can be controlled by the strength and polarity of the applied E-field via E-field controlled CoFeB/MgO interfacial PMA. The demonstrated E-field controlled magnetic-field-sensor based on TMR oscillations may trigger the development of magnetoelectrically controlled magnetic-field-sensor based on MTJs.

[1]W. Eerenstein, N. D. Mathur, and J. F. Scott, Nature (London) **442**, 759 (2006).
[2]Y. Tokura, J. Magn. Magn. Mater. **310**, 1145 (2007).
[3]S. W. Cheong and M. Mostovoy, Nat. Mater. **6**, 13 (2007).
[4]R. Ramesh and N. A. Spaldin, Nat. Mater. **6**, 21 (2007).
[5]J. F. Scott, Nat. Mater. **6**, 256 (2007).
[6]M. Gajek, M. Bibes, S. Fusil, K. Bouzehouane, J. Fontcuberta, A. Barthelemy, and A. Fert, Nat. Mater. **6**, 296 (2007).
[7]W.-G. Wang, M. Li, S. Hageman, and C. L. Chien, Nat. Mater. **11**, 64 (2012).
[8]H. Meng, R. Sbiaa, M. A. K. Akhtar, R. S. Liu, V. B. Naik, and C. C. Wang, Appl. Phys. Lett. **100**, 122405 (2012).
[9]S. Kanai, M. Yamanouchi, S. Ikeda, Y. Nakatani, F. Matsukura, and H. Ohno, Appl. Phys. Lett. **101**, 122403 (2012).
[10]T. Kimura, T. Goto, H. Shintani, K. Ishizaka, T. Arima, and Y. Tokura, Nature **426**, 55 (2003).
[11]Y. Tokunaga, Y. Taguchi, T. Arima, and Y. Tokura, Nat. Phys. **8**, 838 (2012).
[12]M. Fiebig, J. Phys. D: Appl. Phys. **38**, R123 (2005).
[13]J. Ma, J. Hu, Z. Li, and C. W. Nan, Adv. Mater. **23**, 1062 (2011).
[14]N. X. Sun and G. Srinivasan, Spin **2**, 1240004 (2012).
[15]S. Ikeda, K. Miura, H. Yamamoto, K. Mizunuma, H. D. Gan, M. Endo, S. Kanai, J. Hayakawa, F. Matsukura, and H. Ohno, Nat. Mater. **9**, 721 (2010).
[16]D. C. Worledge, G. Hu, David W. Abraham, J. Z. Sun, P. L. Trouilloud, J. Nowak, S. Brown, M. C. Gaidis, E. J. O'Sullivan, and R. P. Robertazzi, Appl. Phys. Lett. **98**, 022501 (2011).
[17]A. Dussaux, B. Georges, J. Grollier, V. Cros, A. Khvalkovskiy, A. Fukushima, M. Konoto, H. Kubota, K. Yakushiji, S. Yuasa, K. Zvezdin, K. Ando, and A. Fert, Nat. Commun. **1**(1), 8 (2010).
[18]H. Sato, M. Yamanouchi, K. Miura, S. Ikeda, H. D. Gan, K. Mizunuma, R. Koizumi, F. Matsukura, and H. Ohno, Appl. Phys. Lett. **99**, 042501 (2011).
[19]T. Nozaki, Y. Shiota, S. Miwa, S. Murakami, F. Bonell, S. Ishibashi, H. Kubota, K. Yakushiji, T. Saruya, A. Fukushima, S. Yuasa, T. Shinjo, and Y. Suzuki, Nat. Phys. **8**(6), 492 (2012).
[20]W. Skowronski, P. Wisniowski, T. Stobiecki, S. Cardoso, P. P. Freitas, and S. van Dijken, Appl. Phys. Lett. **101**, 192401 (2012).
[21]K. Kita, D. W. Abraham, M. J. Gajek, and D. C. Worledge, J. Appl. Phys. **112**, 033919 (2012).
[22]L. E. Fuentes-Cobas, J. A. Matutes-Aquino, and M. E. Fuentes-Montero, *Handbook of Magnetic Materials*, edited by K. H. J. Buschow (Elsevier, North Holland, 2011), Vol. 19, p.161.
[23]R. C. O'Handley, *Modern Magnetic Materials: Principles and Applications* (Wiley, New York, 2000).
[24]N. A. Pertsev, Sci. Rep. **3**, 2757 (2013).
[25]E. Lage, C. Kirchhof, V. Hrkac, L. Kienle, R. Jahns, R. Knöchel, E. Quandt, and D. Meyners, Nat. Mater. **11**, 523 (2012).
[26]V. B. Naik, H. Meng, J. X. Xiao, R. S. Liu, A. Kumar, K. Y. Zeng, P. Luo, and S. Yap, "Effect of electric-field on the perpendicular magnetic anisotropy and strain properties in CoFeB/MgO magnetic tunnel junctions" (unpublished).